Supporting Information for

Chromaticity Coordinates Vector Principle for Charge-Transfer-Type Thermochromic Material Design: Case in Fe/Cr-(co)doped α-Al_2O_3 Host

Wen Zhang [a], Hongda Xu [a], Shan Wang[b*], Hairui Fang [c], Tianyi Li[b], Yumei Zhang [a], Dongfei Li [a], Xiangdong Meng [a*], Changmin Hou [d], Long Yuan [a*]

[a] Key Laboratory of Functional Materials Physics and Chemistry of the Ministry of Education, College of Physics, Jilin Normal University, Changchun 130103, People's Republic of China. Corresponding emails: yuanlong@jlnu.edu.cn (L.Y.); xdmeng@jlnu.edu.cn (X.M.).

[b] Department of Materials Science and Engineering, Jilin Institute of Chemical Technology, 45 Chengde Street, Jilin 132022, People's Republic of China. Corresponding email: wshsmile@hotmail.com (S.W.).

[c] School of Automation Engineering, Northeast Electric Power University, 169 Changchun Road, Jilin 132000, People's Republic of China.

[d] State Key Laboratory of Inorganic Synthesis and Preparative Chemistry, College of Chemistry, Jilin University, 2699 Qianjin Street, Changchun 130012, People's Republic of China.

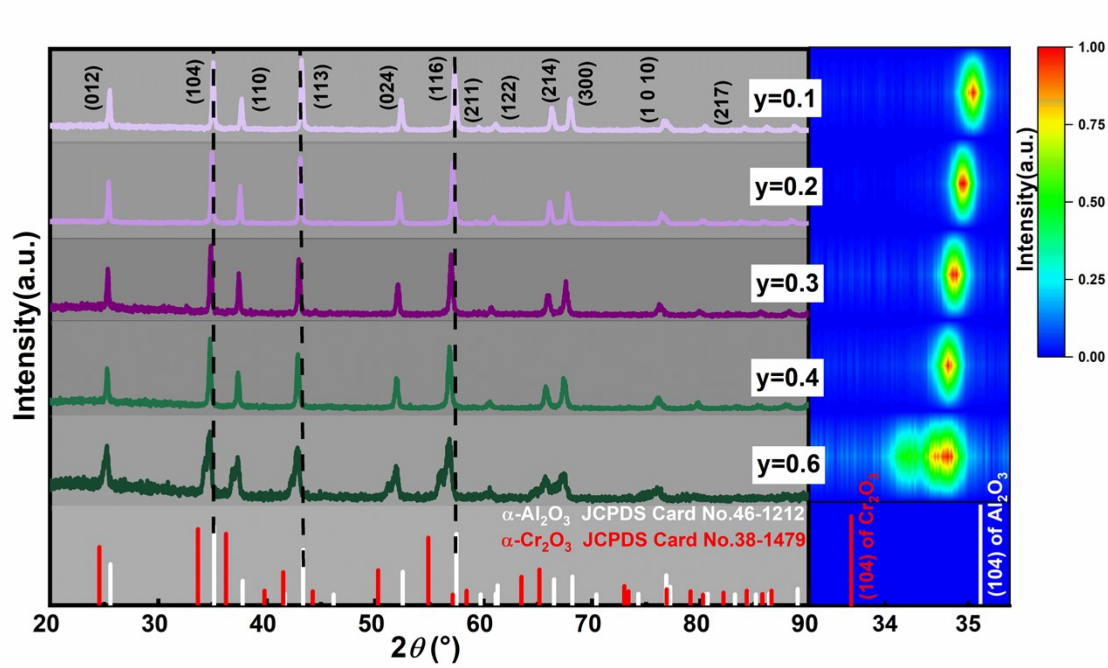

Fig. S1 Powder X-ray diffraction data of the as-synthesized $Al_{2-y}Cr_yO_3$ samples. Vertical bars indicate the theoretical diffraction peak positions and the relative intensities of α-Al_2O_3 (JCPDS Card No. 46-1212) and α-Al_2O_3 (JCPDS Card No. 38-1479). Dash lines mark the peak positions as a guide for the eye. Right panel depicts the contour maps of (104) diffraction peaks for different samples.

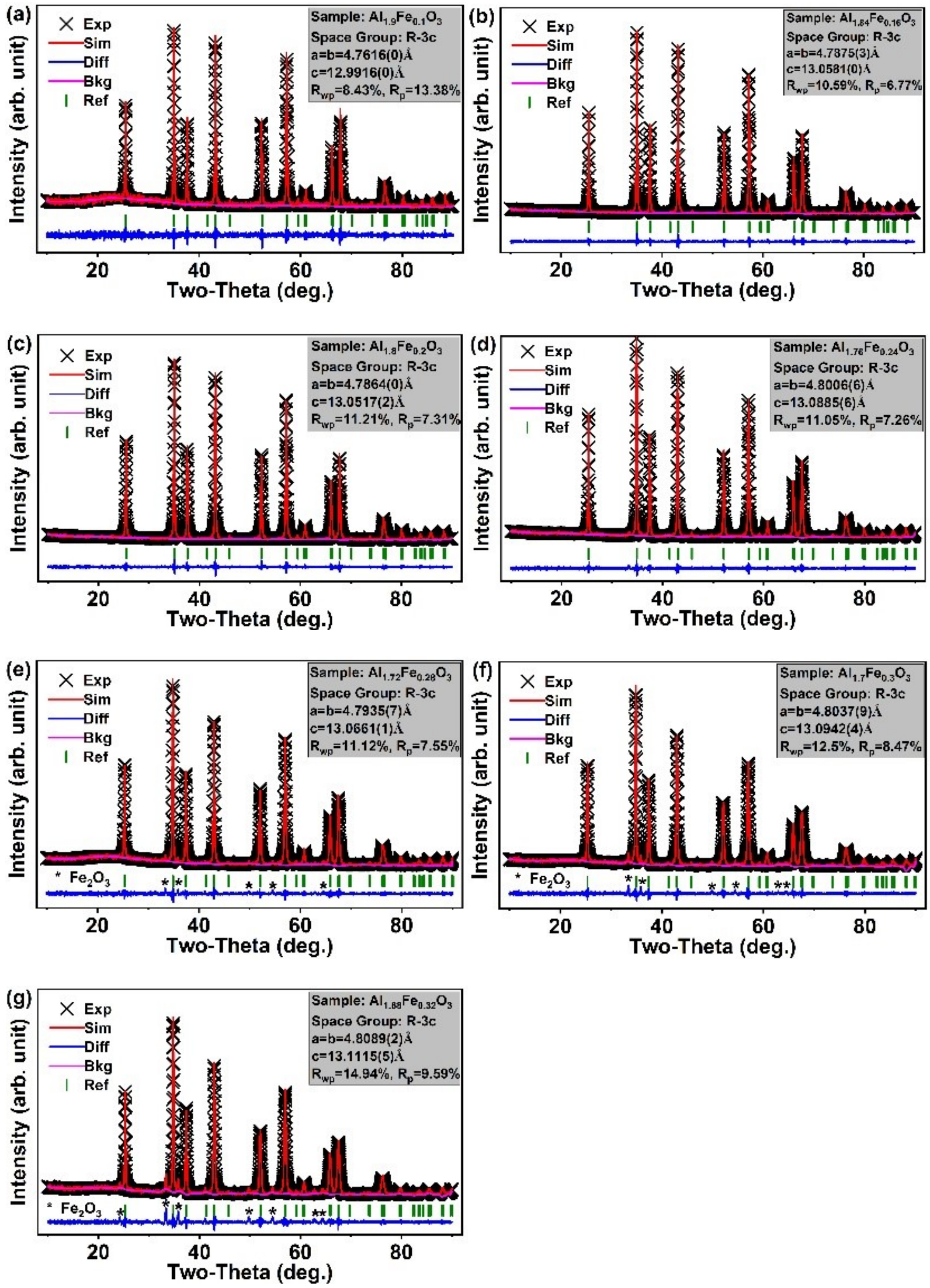

Fig. S2 Rietveld refinement results of the powder x-ray diffraction data of $Al_{2-x}Fe_xO_3$ samples for (a) x=0.10, (b) x=0.16, (c) x=0.20, (d) x=0.24, (e) x=0.28, (f) x=0.30, and (g) x=0.32, respectively.

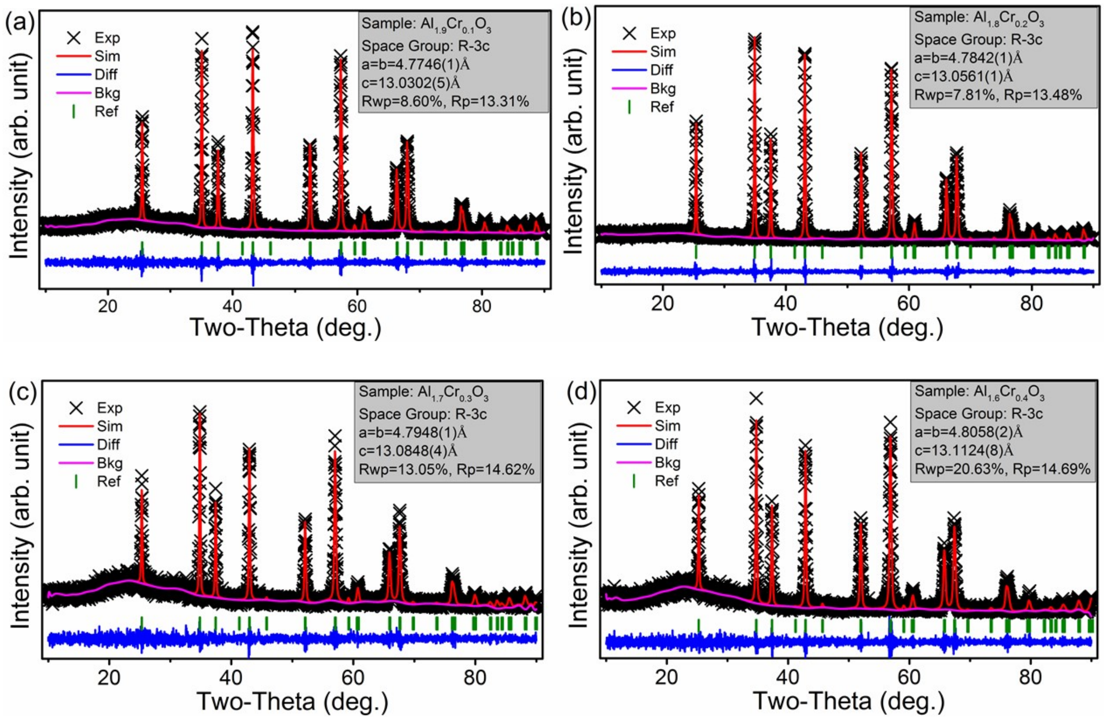

Fig. S3 Rietveld refinement results of the powder x-ray diffraction data of $Al_{2-y}Cr_yO_3$ samples for (a) y=0.10, (b) y=0.20, (c) y=0.30, (d) y=0.40, respectively.

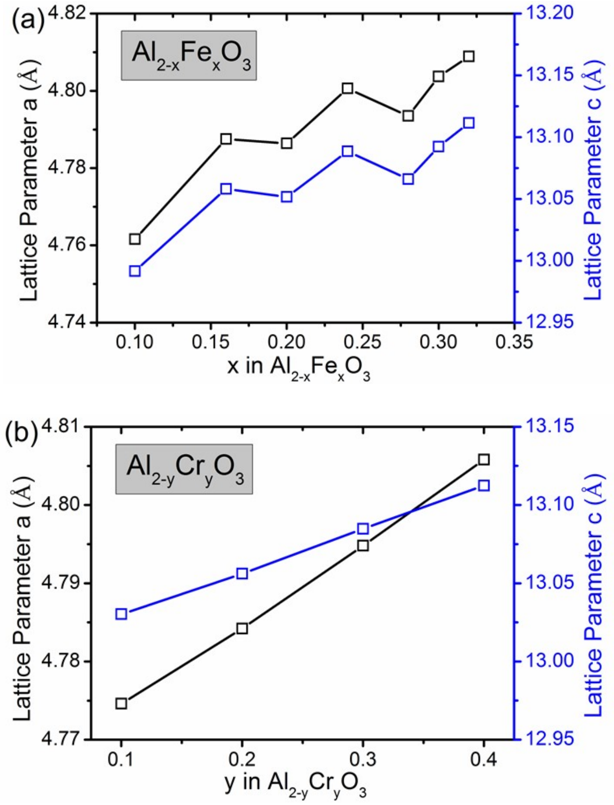

Fig. S4 Lattice parameters as a function of the doping levels of (a) x in $Al_{2-x}Fe_xO_3$ and (b) y in $Al_{2-y}Cr_yO_3$.

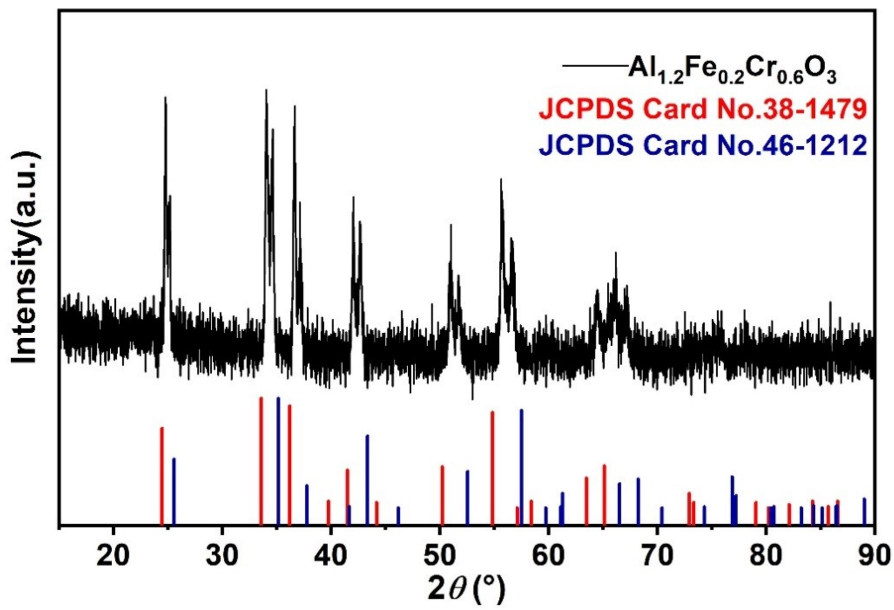

Fig. S5 Powder X-ray diffraction data of $Al_{1.2}Fe_{0.2}Cr_{0.6}O_3$. vertical bars indicate the peak position and theoretical intensities of the JCPDS Card No. 46-1212 (blue) and 38-1479 (red) for Al_2O_3 and Cr_2O_3 respectively.

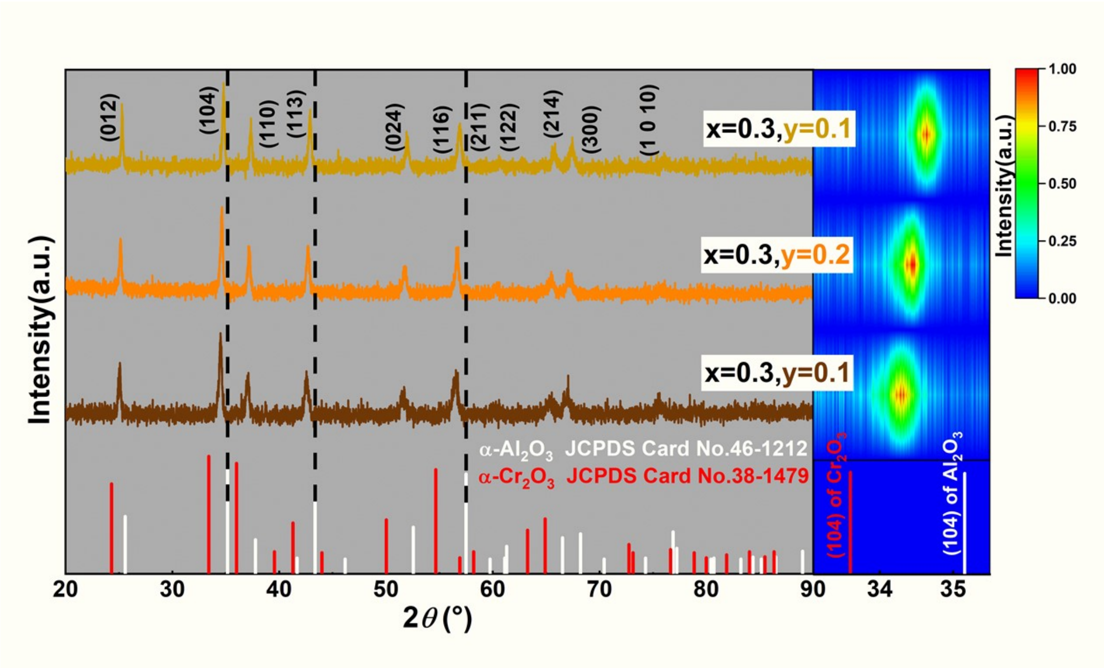

Fig. S6 Powder X-ray diffraction data of the as-synthesized $Al_{1.7-y}Fe_{0.3}Cr_yO_3$ samples. Vertical bars indicate the theoretical diffraction peak positions and the relative intensities of α-Al_2O_3 (JCPDS Card No. 46-1212) and α-Al_2O_3 (JCPDS Card No. 38-1479). Dash lines mark the peak positions as a guide for the eye. Right panel depicts the contour maps of (104) diffraction peaks for different samples.

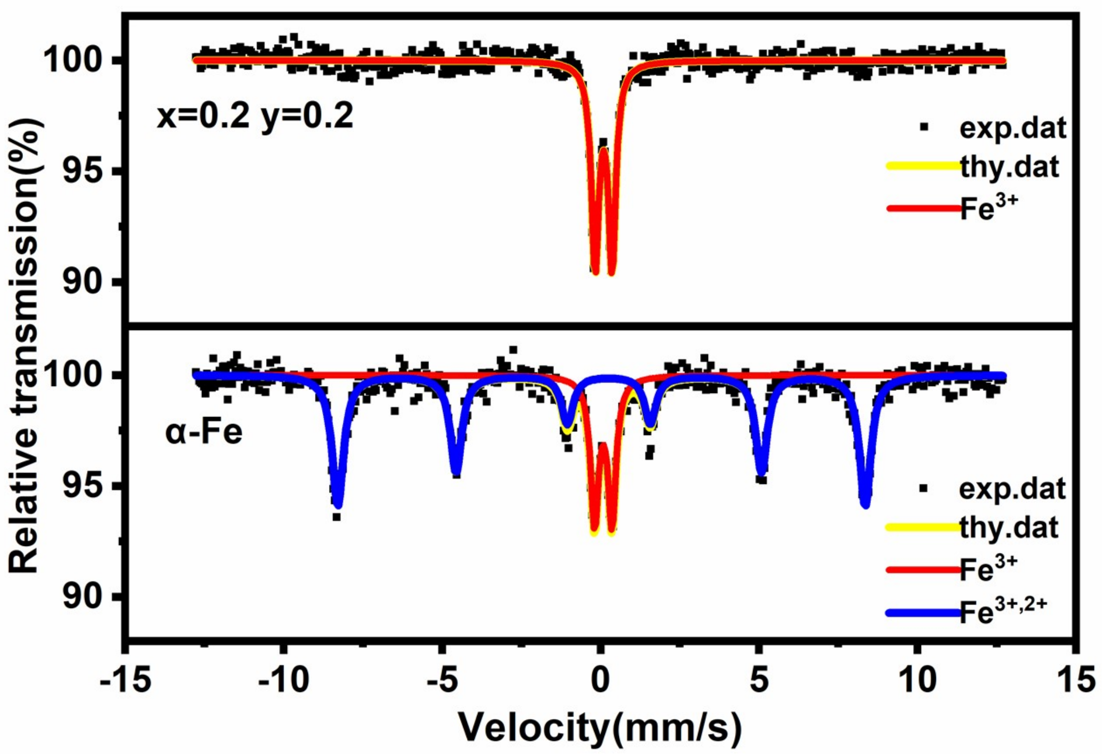

Fig. S7 Mössbauer spectra of $Al_{1.6}Fe_{0.2}Cr_{0.2}O_3$ and the standard α-Fe sample as a reference.

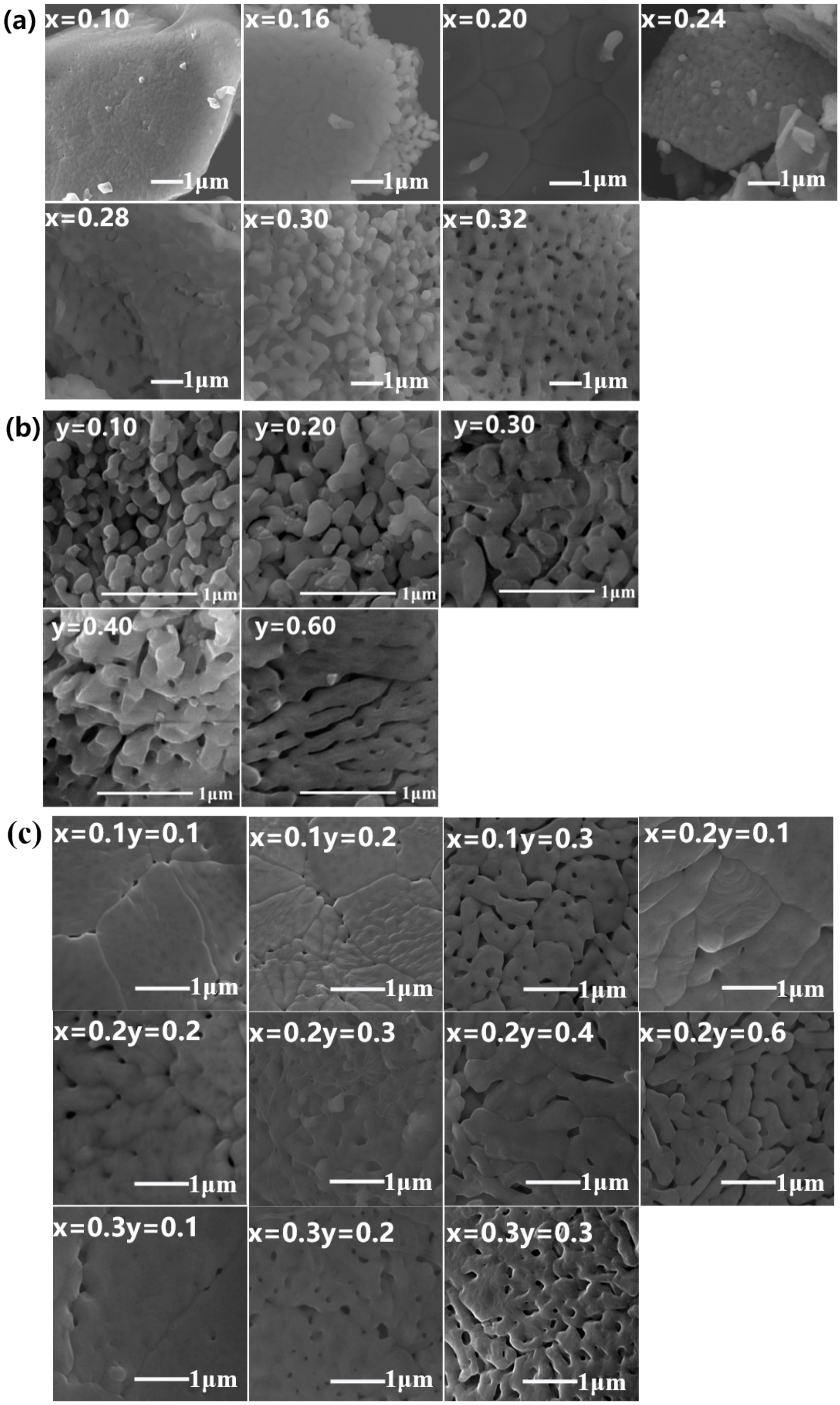

Fig. S8 SEM graphs of the as-synthesized samples (a) $Al_{2-x}Fe_xO_3$ (x=0.10, 0.16, 0.20, 0.24, 0.28, 0.30, 0.32), (b) $Al_{2-y}Cr_yO_3$ (y=0.1, 0.2, 0.3, 0.4, 0.6), (c) $Al_{2-x}Fe_xCr_yO_3$ (x=0.1, 0.2, 0.3; y=0.1, 0.2, 0.3, 0.4, 0.6).

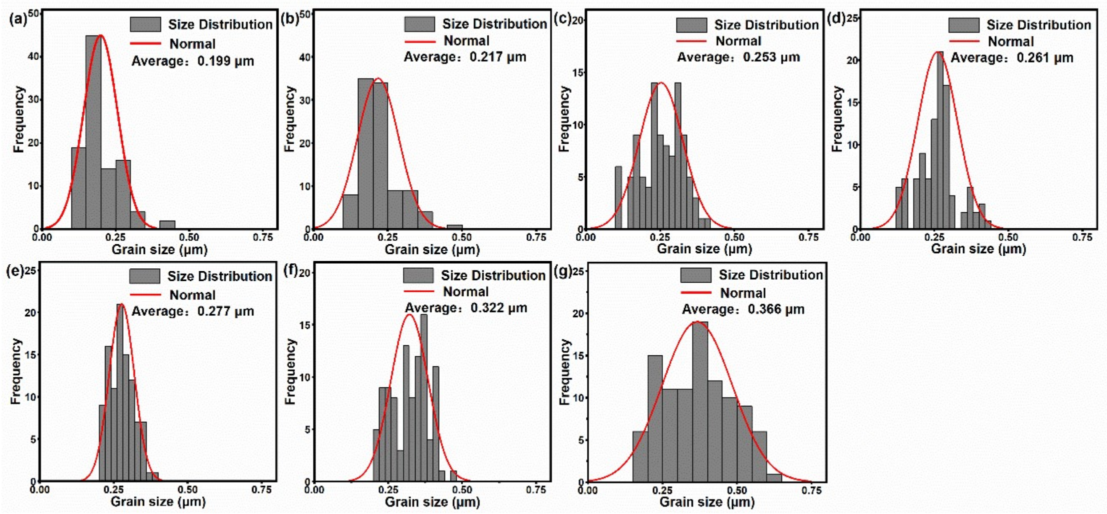

Fig. S9 Histogram graphs of the particle size distribution of the samples $Al_{2-x}Fe_xO_3$(x=0.10-0.32), (a)x=0.10, (b) x=0.16, (c) x=0.20, (d) x=0.24, (e) x=0.28, (f) x=0.30, (g) x=0.32.

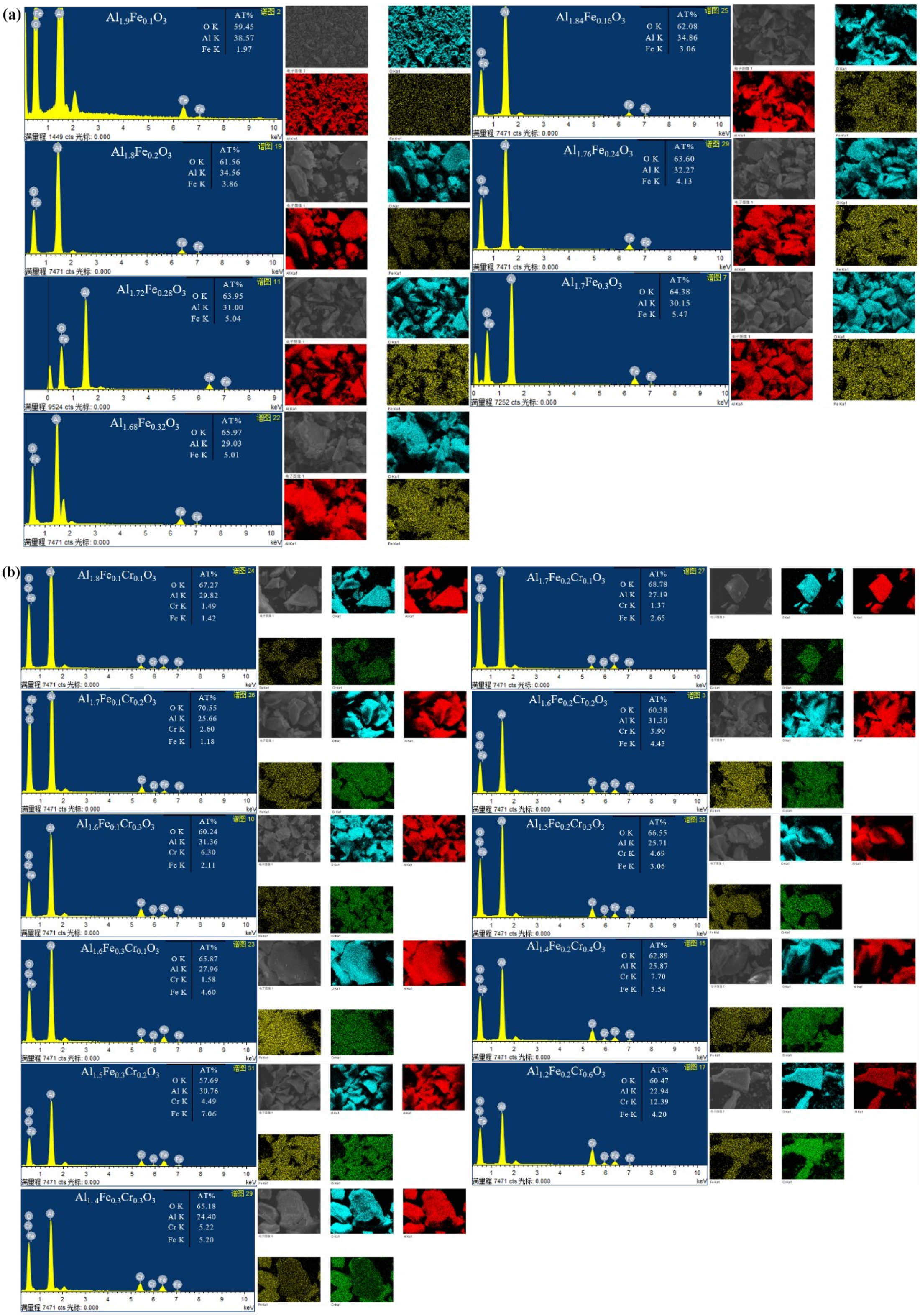

Fig. S10 EDS and element distribution mapping graphs of the samples (a) $Al_{2-x}Fe_xO_3$ (x=0.1, 0.16, 0.20, 0.24, 0.28, 0.30, 0.32), (b) $Al_{2-x}Fe_xCr_yO_3$ (x=0.1, 0.2, 0.3; y=0.1, 0.2, 0.3, 0.4, 0.6). In the mapping graphs, O cyan, Al red, Fe yellow, and Cr green. Tables in each diagram listed the measured atomic ratio from the integration of the area of each elements in the EDS for the samples with varied stoichiometry.

Table S1. EDS results of atomic percentage and theoretical vs. experimental Al/Fe ratio in as-synthesized $Al_{2-x}Fe_xO_3$ samples.

$Al_{2-x}Fe_xO_3$	Atomic ratio (%)			Theoretical value of Fe/Al	Experimental value of Fe/Al
	Fe	Al	O		
x=0.10	1.97	38.57	59.45	0.052	0.051
x=0.16	3.06	34.86	62.08	0.087	0.088
x=0.20	3.86	34.56	61.56	0.111	0.112
x=0.24	4.13	32.27	63.60	0.136	0.128
x=0.28	5.04	31.00	63.95	0.163	0.162
x=0.30	5.47	30.15	64.38	0.176	0.181
x=0.32	5.01	29.03	65.97	0.190	0.173

Table S2. EDS results of atomic percentage and theoretical vs. experimental Al/Fe and Al/Cr ratio in as-synthesized $Al_{2-x-y}Fe_xCr_yO_3$ samples.

$Al_{2-x-y}Fe_xCr_yO_3$	Atomic ratio (%)				Theoretical value of Fe/Al	Experimental value of Fe/Al	Theoretical value of Cr/Al	Experimental value of Cr/Al
	Fe	Cr	Al	O				
x=0.1, y=0.1	1.42	1.49	29.82	67.27	0.056	0.048	0.056	0.050
x=0.1, y=0.2	1.18	2.60	25.66	70.55	0.059	0.046	0.118	0.101
x=0.1, y=0.3	2.11	6.30	31.36	60.24	0.063	0.067	0.188	0.201
x=0.2, y=0.1	2.65	1.37	27.19	68.78	0.118	0.097	0.059	0.050
x=0.2, y=0.2	4.43	3.90	31.30	60.38	0.125	0.142	0.125	0.125
x=0.2, y=0.3	3.06	4.69	25.71	66.55	0.133	0.119	0.200	0.182
x=0.3, y=0.1	4.60	f1.58	27.96	65.87	0.188	0.165	0.063	0.057
x=0.3, y=0.2	7.06	4.49	30.76	57.69	0.200	0.230	0.133	0.146
x=0.3, y=0.3	5.20	5.22	24.40	65.18	0.214	0.213	0.214	0.214

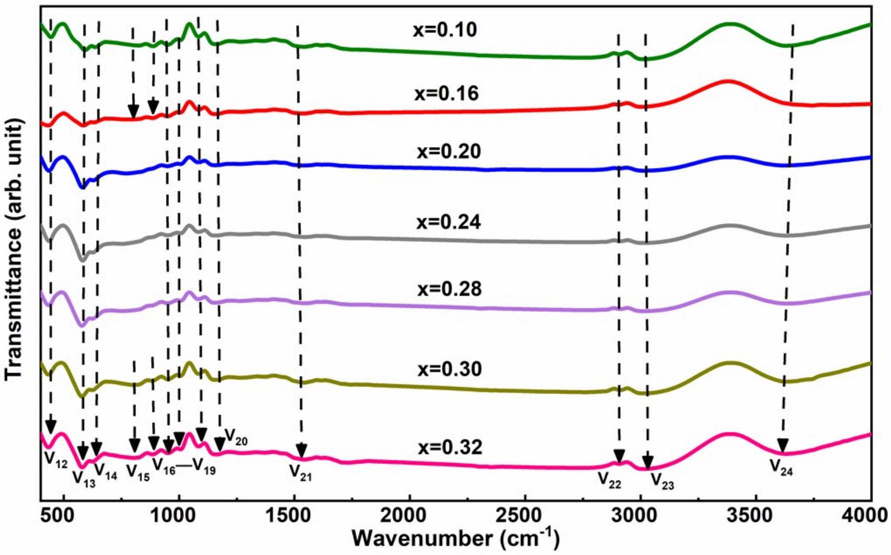

Fig. S11 Infrared spectra of $Al_{2-x}Fe_xO_3$ samples in the wavenumber range of 400-4000 cm^{-1}.

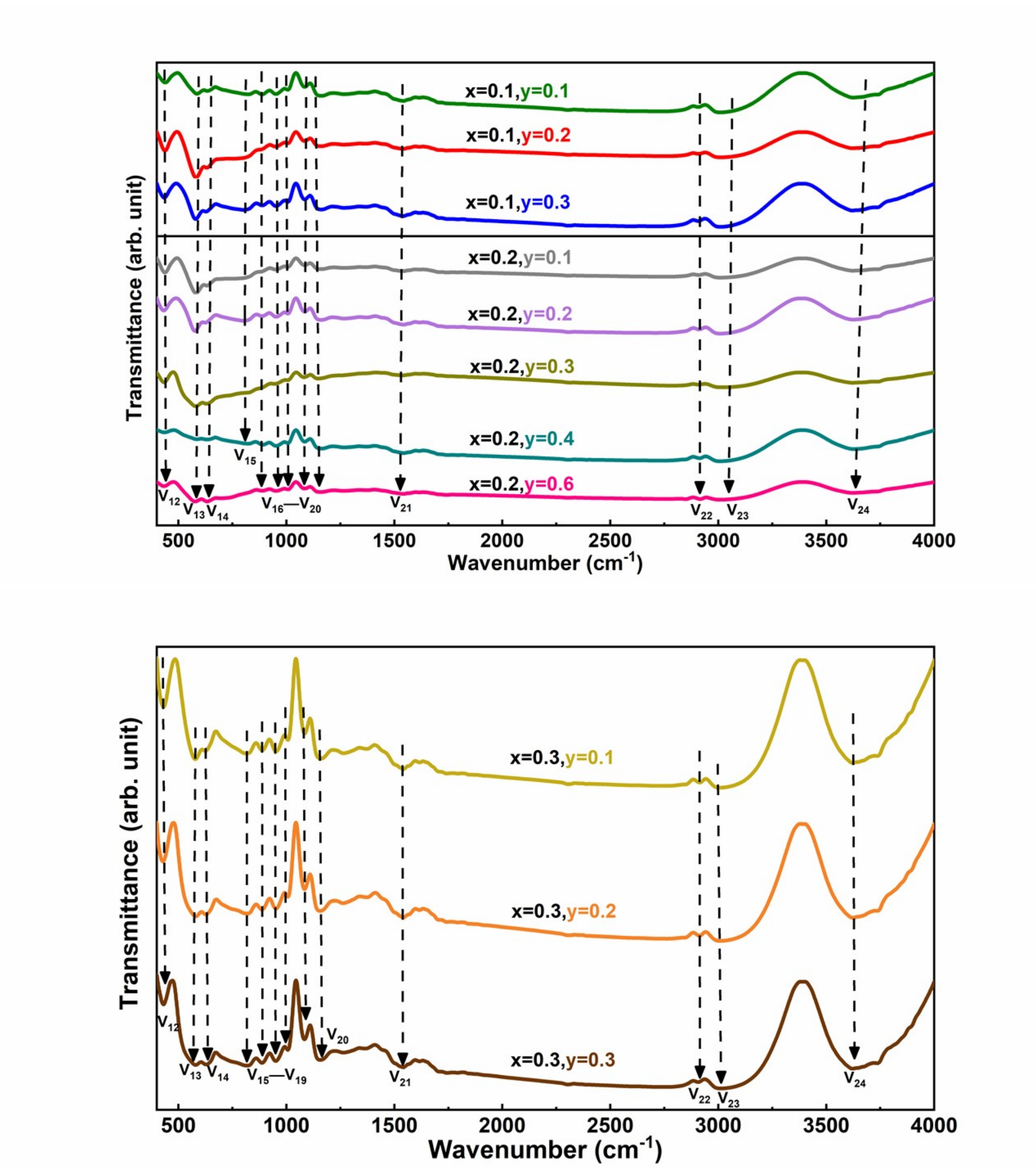

Fig. S12 Infrared spectra of $Al_{2-x-y}Fe_xCr_yO_3$ samples in the range of 400-4000 cm^{-1}.

Table S3. Assignment of the Raman vibration modes of $Al_{2-x}Fe_xO_3$ and $Al_{2-x-y}Fe_xCr_yO_3$ samples with varied doping levels

	peak position of the vibration modes in Raman spectra (cm^{-1})									
	V_1(Fe)	V_2(Fe)	V_3(Al)	V_4(Al)	V_5(Al)	V_6(Fe)	V_7(Al)	V_8(Fe)	V_9(Al)	V_{10}(Al)
	A_{1g}	E_g	E_g	A_{1g}	E_g	A_{1g}	E_g	E_g	A_{1g}	E_g
x=0.10	-	-	378	414	434	-	577	609	651	750
x=0.16	-	-	379	415	452	-	566	616	633	751
x=0.20	-	-	377	418	474	-	563	628	661	753
x=0.24	236	302	-	415	-	500	560	627	672	741
x=0.28	234	302	-	418	-	509	555	628	667	740
x=0.30	234	301	-	415	-	506	555	624	682	748
x=0.32	233	300	-	417	-	510	555	618	672	-
x=0.1,y=0.	-	-	361	-	-	503	-	-	-	
x=0.1,y=0.	-	-	372	-	-	492	577	617	-	785
x=0.1,y=0.	-	-	376	-	-	500	577	621	662	758
x=0.2,y=0.	235	-	381	405	431	507	560	619	664	755
x=0.2,y=0.	230	-	389	409	425	492	550	612	652	743
x=0.2,y=0.	234	-	386	408	436	498	554	599	647	728
x=0.2,y=0.	245	-	394	406	426	496	570	597	660	737
x=0.2,y=0.	265	-	392	402	430	505	572	599	652	730
x=0.3,y=0.	237	-	331	403	423	488	542	583	676	766
x=0.3,y=0.	264	-	335	400	453	498	542	619	640	727
x=0.3,y=0.	234	-	338	402	469	501	578	617	645	715

Table S4. Peaks of FT-IR transmission spectroscopy of the $Al_{2-x}Fe_xO_3$ and $Al_{2-x-y}Fe_xCr_yO_3$ samples

	V_{12}	V_{13}	V_{14}	V_{15}	V_{16}	V_{17}	V_{18}	V_{19}	V_{20}	V_{21}	V_{22}	V_{23}	V_{24}
	Al-O	Fe-O	Al-O Cr-O	Fe-O	Fe-O								
x=0.10	435	592	636	825	888	950	1007	1084	1159	1542	2909	3013	3628
x=0.16	433	585	631	834	884	951	1006	1085	1159	1543	2907	3010	3625
x=0.20	436	582	628	-	-	950	1006	1084	1156	1543	2907	3013	3629
x=0.24	437	582	625	-	-	951	1007	1085	1158	1544	2914	3010	3632
x=0.28	435	579	624	-	-	950	1007	1084	1156	1544	2914	3012	3632
x=0.30	434	579	624	804	883	951	1007	1085	1158	1543	2913	3011	3627
x=0.32	434	580	624	803	885	951	1007	1085	1162	1543	2907	3012	3631
x=0.1,y=0.	440	586	634	824	888	952	1007	1085	1162	1542	2907	3000	3628
x=0.1,y=0.	438	582	632	803	889	950	1007	1084	1158	1542	2909	3011	3623
x=0.1,y=0.	435	580	628	802	888	952	1007	1085	1162	1543	2924	-	3430
x=0.2,y=0.	438	582	632	828	889	952	1007	1085	1161	1542	2910	3010	3621
x=0.2,y=0.	432	577	624	803	888	953	1007	1085	1162	1543	2911	3010	3627
x=0.2,y=0.	434	581	631	816	889	954	1005	1082	1148	1542	2909	3015	3622
x=0.2,y=0.	434	586	634	824	891	953	1007	1085	1160	1543	2913	3001	3628
x=0.2,y=0.	433	577	634	-	888	953	1008	1084	1158	1542	2917	3009	3623
x=0.3,y=0.	431	578	625	820	888	952	1007	1085	1159	1617	2914	3009	3623
x=0.3,y=0.	429	581	627	821	887	952	1007	1084	1156	1543	2913	3009	3624
x=0.3,y=0.	431	580	628	821	887	951	1007	1084	1156	1542	2907	3011	3622

Table S5. The CIE-L*a*b* numerical value results of $Al_{2-x}Fe_xO_3$ with varied Fe-doping levels

x	x=0.10			x=0.16			x=0.20			x=0.24			x=0.28			x=0.30			x=0.32		
T	L*	a*	b*	L*	a*	b*	L*	a*	b*	L*	a*	b*	L*	a*	b*	L*	a*	b*	L*	a*	b*
50°C	76	3	18	78	5	30	70	10	36	63	21	39	53	30	39	47	31	32	46	44	45
75°C	76	3	20	75	5	31	71	10	36	61	20	36	52	30	37	52	31	33	46	44	44
100°C	77	3	20	75	6	35	70	9	40	60	22	37	46	31	38	50	30	34	44	43	43
125°C	73	3	19	70	4	34	62	11	39	47	21	36	40	31	43	46	28	33	35	40	49
150°C	75	4	20	67	5	38	59	11	37	47	21	37	38	29	40	49	26	27	31	38	44
175°C	74	3	19	69	5	36	59	12	41	51	22	42	40	30	47	45	25	27	34	39	44
200°C	75	3	21	72	4	37	64	10	41	51	18	39	45	29	44	48	26	27	36	38	44
225°C	76	3	19	72	3	36	62	10	42	52	20	37	42	28	40	46	23	23	33	36	39
250°C	74	4	24	67	5	29	60	9	31	52	16	30	43	23	32	41	24	28	36	33	33
275°C	75	3	20	66	4	28	58	8	30	51	15	28	42	22	32	43	22	25	36	30	31
300°C	71	3	20	61	4	39	52	9	35	46	17	33	36	21	34	33	20	19	30	29	33
325°C	74	3	20	58	6	36	49	10	30	44	18	31	31	21	29	40	20	21	27	26	29
350°C	74	3	21	62	3	27	58	7	27	51	13	24	43	16	23	39	18	21	37	21	20
375°C	71	3	21	64	6	28	57	9	27	52	13	23	41	17	23	34	16	14	37	20	19
400°C	73	3	21	62	6	34	50	9	34	40	15	26	28	16	22	39	16	18	27	19	20
425°C	73	2	22	72	5	28	64	7	27	57	13	25	38	12	21	41	14	19	28	18	18
450°C	69	3	22	66	5	38	52	11	35	47	12	29	34	15	24	31	14	16	25	17	17
475°C	68	3	21	65	5	30	54	9	33	42	13	24	26	15	20	27	12	14	18	17	14
500°C	67	3	23	73	6	35	60	7	34	49	12	27	33	13	22	34	13	17	32	18	21
525°C	66	3	21	65	4	28	58	8	29	53	10	23	36	12	17	25	10	11	34	14	16
550°C	68	3	22	74	4	37	62	9	38	54	12	30	40	13	25	32	12	14	31	14	19

Table S6. The CIE-L*a*b* numerical value results of $Al_{2-y}Cr_yO_3$ with varied Cr-doping levels

T \ y	y=0.1			y=0.2			y=0.3			y=0.4			y=0.6		
	L*	a*	b*	L*	a*	b*	L*	a*	b*	L*	a*	b*	L*	a*	b*
50°C	53	4	-1	52	10	-3	47	5	-1	46	1	0	42	-7	5
75°C	52	3	0	52	8	1	47	5	-1	44	0	1	43	-8	7
100°C	54	3	1	53	7	0	49	3	1	44	-1	3	43	-9	7
125°C	45	2	0	49	5	1	43	3	1	40	-2	2	35	-8	7
150°C	47	1	0	51	3	1	45	0	1	42	-4	3	41	-10	6
175°C	49	2	-1	50	2	0	44	0	1	42	-3	2	37	-10	6
200°C	48	2	0	52	3	1	47	-1	3	43	-5	5	41	-10	7
225°C	49	1	0	52	1	0	45	-2	2	44	-5	3	42	-8	6
250°C	45	0	-1	47	-1	3	43	-5	5	39	-5	4	35	-10	9
275°C	54	1	0	51	0	1	45	-4	3	40	-5	3	39	-9	7
300°C	44	0	1	44	0	1	35	-4	3	35	-5	4	35	-9	7
325°C	49	0	1	51	-2	3	45	-4	3	43	-6	6	42	-12	9
350°C	46	-1	3	49	-1	3	42	-4	4	41	-6	6	35	-7	5
375°C	50	-1	3	49	-2	5	47	-6	5	41	-7	5	40	-10	9
400°C	42	1	4	50	-3	4	43	-2	3	40	-6	7	38	-9	8
425°C	50	2	3	49	-2	5	39	-2	5	43	-8	7	32	-9	9
450°C	44	0	3	45	-3	5	38	-5	5	34	-6	6	32	-5	7
475°C	38	0	1	43	-2	5	31	-3	5	32	-7	6	34	-7	8
500°C	41	-1	3	47	-4	8	40	-6	7	39	-7	8	33	-9	9
525°C	35	-2	4	44	-5	5	31	-5	4	34	-5	7	33	-9	9
550°C	38	0	3	44	-3	5	40	-6	7	35	-6	6	30	-9	7

Table S7. The CIE-L*a*b* values of $Al_{2-x-y}Fe_xCr_yO_3$ with varied Fe,Cr co-doping levels

x,y / T	0.1,0.1	0.1,0.2	0.1,0.3	0.2,0.1	0.2,0.2	0.2,0.3	0.2,0.4	0.2,0.6	0.3,0.1	0.3,0.2	0.3,0.3
	L*,a*,b*	L*,a*,b*	L*,a*,b*	L*,a*,b*	L*,a*,b*	L*,a*,b*	L*,a*,b*	L*,a*,b*	L*,a*,b*	L*,a*,b*	L*,a*,b*
50°C	51,6,24	34,5,17	30,2,16	34,6,21	27,4,18	18,3,11	16,2,10	11,1,5	24,11,13	18,7,10	16,5,9
75°C	54,6,25	40,4,20	30,3,20	34,8,21	27,4,18	19,3,11	11,1,9	11,1,5	23,9,13	18,7,9	18,5,9
100°C	45,4,24	30,3,17	25,3,14	33,6,21	26,4,18	16,2,12	9,2,5	9,0,4	21,9,13	15,7,9	19,5,9
125°C	43,4,25	31,3,21	23,4,21	32,6,30	26,5,23	15,5,15	11,3,9	7,1,4	21,13,21	15,6,12	11,9,9
150°C	40,4,27	28,2,19	21,4,18	32,5,28	25,5,24	11,3,11	11,2,10	5,2,2	19,11,19	14,6,12	10,5,7
175°C	46,5,26	26,1,22	24,2,23	26,4,27	22,5,22	8,3,7	9,3,7	3,2,2	14,8,15	6,3,4	7,3,6
200°C	50,5,27	38,2,20	24,3,22	23,6,24	19,4,17	11,2,10	8,4,6	4,3,1	14,8,15	13,7,10	15,7,9
225°C	45,6,25	34,1,21	22,3,20	22,5,23	17,4,19	9,4,9	8,3,4	3,2,2	14,10,15	10,5,9	9,6,7
250°C	46,3,23	32,1,17	28,3,17	34,5,26	29,4,23	21,5,14	13,3,9	6,2,3	20,9,13	17,7,11	10,5,9
275°C	44,2,21	28,1,18	27,3,18	34,5,26	32,7,26	22,5,13	12,3,8	7,1,4	23,11,14	18,7,11	14,5,7
300°C	40,4,24	25,2,21	22,4,17	29,6,29	21,6,25	11,3,9	8,3,8	4,2,2	18,8,15	9,5,8	6,4,5
325°C	42,4,26	29,2,21	19,4,17	28,7,27	19,6,21	12,5,10	10,3,9	4,1,3	13,8,15	11,7,9	10,5,7
350°C	52,2,23	38,0,18	33,3,16	42,5,23	40,4,20	22,4,11	26,3,9	21,2,5	29,7,14	22,7,8	20,4,7
375°C	51,2,22	36,1,17	34,3,17	37,6,21	35,5,18	29,3,12	25,3,9	22,1,7	27,8,10	23,6,9	21,3,6
400°C	40,2,23	29,0,16	23,3,15	22,6,19	30,6,19	16,3,10	11,2,4	10,2,3	19,3,13	13,7,8	11,5,6
425°C	44,1,20	33,1,14	26,2,15	32,6,18	32,5,15	23,2,11	20,3,6	15,0,5	21,7,12	22,7,8	19,4,8
450°C	48,4,26	29,1,17	26,5,16	30,6,21	21,7,17	22,3,11	10,3,4	12,2,6	21,7,11	13,7,9	13,6,7
475°C	42,1,24	24,1,15	23,3,14	23,5,16	23,5,15	12,5,7	10,1,5	17,6,12	20,7,11	11,6,6	11,4,6
500°C	45,2,24	32,0,16	28,3,14	29,5,22	26,5,16	17,3,10	14,3,8	12,5,4	25,5,12	19,5,9	16,4,4
525°C	46,1,20	31,1,14	26,3,12	31,5,19	27,5,14	18,4,7	17,2,5	12,2,3	23,8,8	16,6,5	15,5,6
550°C	50,3,28	35,0,20	28,4,15	26,5,16	23,4,15	12,3,6	11,1,6	9,0,2	18,7,10	11,5,4	10,5,3

Table S8 Assignments of the absorption bands of $Al_{2-x}Fe_xO_3$ samples.

x	$^6A_{1g}\rightarrow{}^4T_{1g}(^4P)$	$^6A_{1g}\rightarrow{}^4E_g(^4D)$	$^6A_{1g}\rightarrow{}^4E_g, {}^4A_{1g})$	$2(^6A_{1g})\rightarrow 2[^4T_{1g}(^4G)]$
x=0.10	259	378	455	527
x=0.16	274	382	456	531
x=0.20	274	382	457	531
x=0.24	281	387	457	532
x=0.28	298	388	463	535
x=0.30	300	386	450	538
x=0.32	301	390	464	545

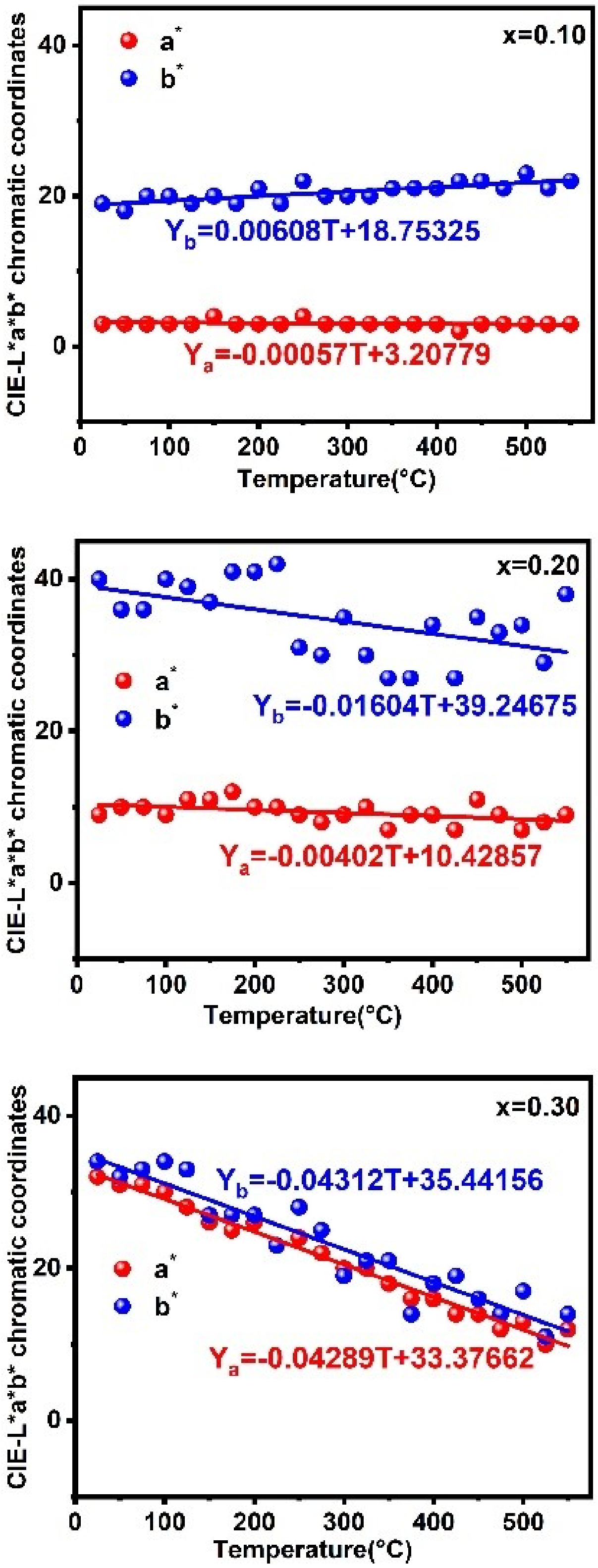

Fig. S13 Chromatic coordinates of a* and b* as a function of temperature for the $Al_{2-x}Fe_xO_3$ samples with x=0.10, 0.20, and 0.30, respectively.

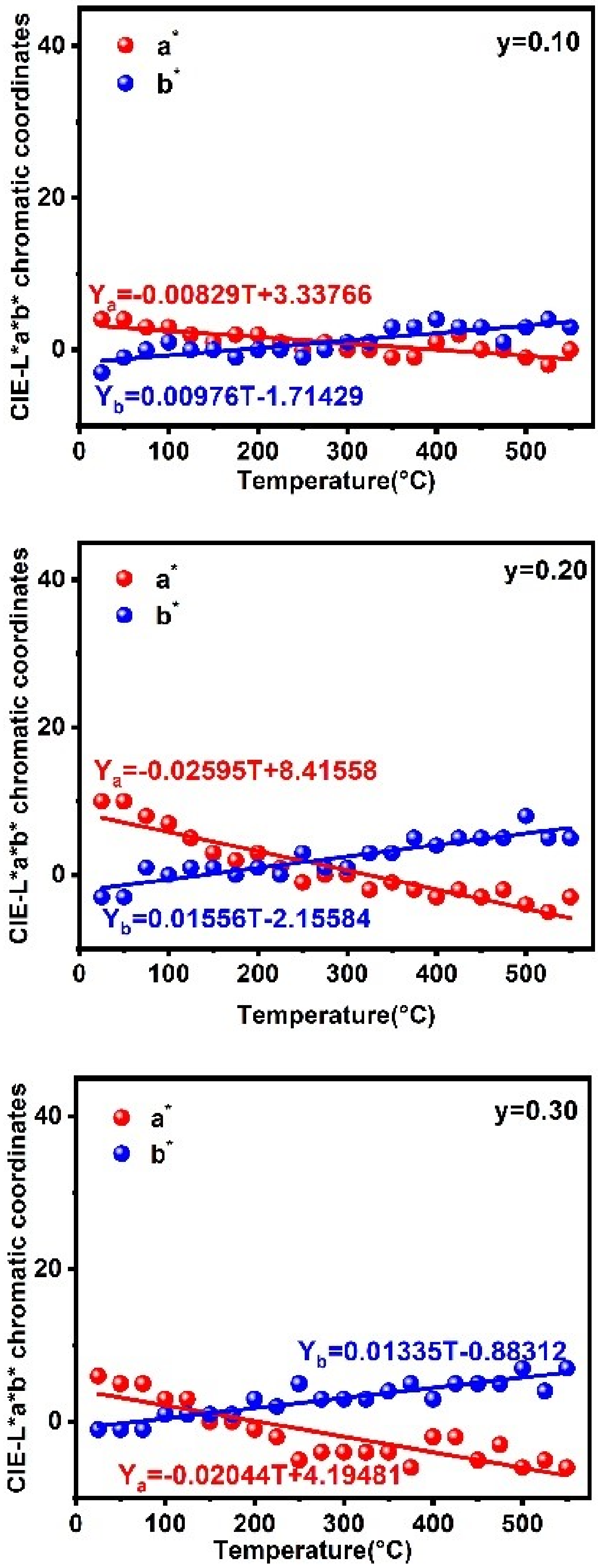

Fig. S14 Chromatic coordinates of a* and b* as a function of temperature for the $Al_{2-y}Cr_yO_3$ samples with y=0.10, 0.20, and 0.30, respectively.

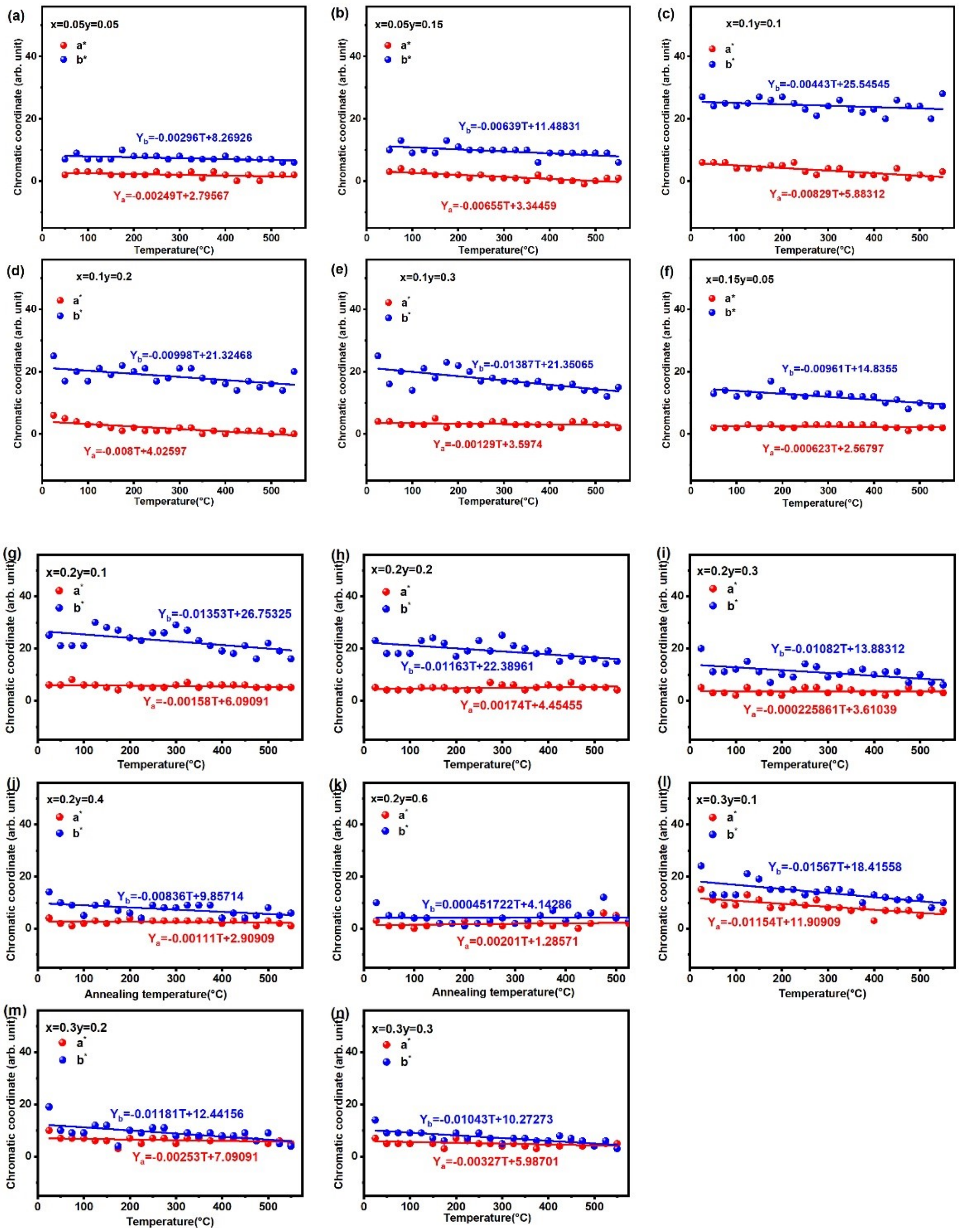

Fig. S15 Chromatic coordinates of a* and b* as a function of temperature for the $Al_{2-x-y}Fe_xCr_yO_3$ samples with x=0.05, 0.1, 0.15, 0.2, 0.3 and y=0.05, 0.1, 0.15, 0.2, 0.3, 0.4, 0.6, respectively.

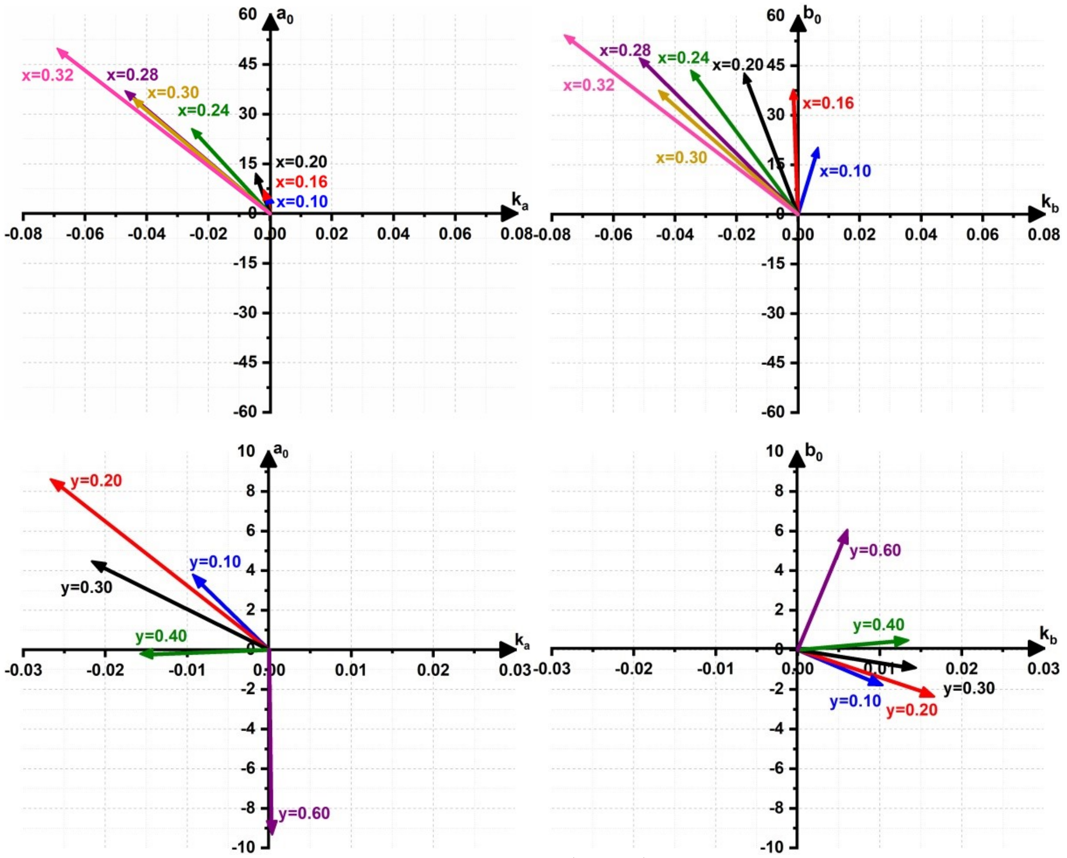

Fig. S16 Thermochromic coordinate vectors of the $\vec{a}$ and $\vec{b}$ of $Al_{2-x}Fe_xO_3$ and $Al_{2-y}Cr_yO_3$ materials.

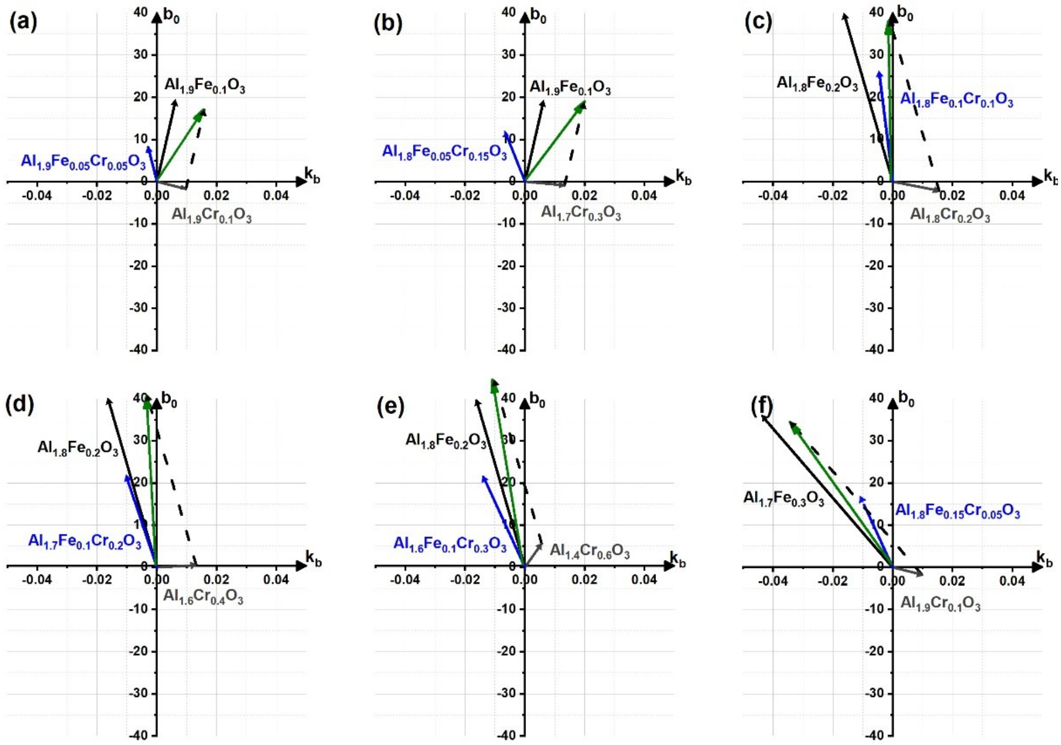

Fig. S17 (a)-(f) The fitting line of the color coordinate b-value function corresponding to different doping ratios. The black line is Fe doped Al_2O_3, the gray line is Cr doped Al_2O_3, the blue line is Fe Cr co-doped Al_2O_3, and the green line It is obtained by doing vector lines for black and gray.